Science of the Total Environment 900 (2023) 165320

Contents lists available at ScienceDirect

Science of the Total Environment

journal homepage: www.elsevier.com/locate/scitotenv

Development of nature-based sustainable passive technologies for treating and disinfecting municipal wastewater: Experiences from constructed wetlands and slow sand filter

Yamini Mittal [a,b], Pratiksha Srivastava [c], Sony Pandey [a,b], Asheesh Kumar Yadav [a,b,*]

[a] CSIR-Institute of Minerals and Materials Technology, Bhubaneswar, Odisha 751013, India
[b] Academy of Scientific and Innovative Research (AcSIR), Ghaziabad, 201002, India
[c] Department of Chemical and Environmental Technology, Rey Juan Carlos University, Móstoles, Madrid, Spain

ARTICLE INFO

Editor: Jan Vymazal

Keywords:
Disinfection
Municipal wastewater treatment
Constructed wetland
Constructed wetland integrated microbial fuel cell
Slow sand filter
Reuse

ABSTRACT

There is an urgent need to develop low-cost technology for effective wastewater treatment and its further disinfection to the level that makes it economically useful. This work has designed and evaluated the various types of constructed wetlands (CWs) followed by a slow sand filter (SSF) for wastewater treatment and disinfection. The studied CWs were, CWs with gravels (CW-G), free water surface-CW (FWS-CWs), and CWs integrated microbial fuel cell (MFC) with granular graphite (CW-MFC-GG) planted with *Canna indica* plant species. These CWs were operated as secondary wastewater treatment technologies followed by SSF for disinfection purposes. The highest total coliform removal was observed in the combination of CW-MFC-GG-SSF which achieved a final concentration of 172 CFU/100 mL, whereas faecal coliform removal was 100 % with the combinations of CW-G-SSF and CW-MFC-GG-SSF, achieving 0 CFU/100 mL in the effluent. In contrast, FWS-SSF achieved the lowest total and faecal coliform removal attaining a final concentration of 542 CFU/100 mL and 240 CFU/100 mL, respectively. Furthermore, *E. coli* were detected as negative/absent in CW-G-SSF and CW-MFC-GG-SSF, while it was positive for FWS-SSF. In addition, the highest turbidity removal was achieved in CW-MFC-GG and SSF combination of 92.75 % from the municipal wastewater influent turbidity of 82.8 NTU. Furthermore, in terms of overall treatment performance of CW-G-SSF and CW-MFC-GG-SSF, these systems were able to treat 72.7 ± 5.5 % and 67.0 ± 2.4 % of COD and 92.3 % and 87.6 % of phosphate, respectively. Additionally, CW-MFC-GG also exhibited a power density of 85.71 mA/m^3 and a current density of 25.71 mW/m^3 with 700 Ω of internal resistance. Thus, CW-G and CW-MFC-GG followed by SSF could be a promising solution for enhanced disinfection and wastewater treatment.

1. Introduction

Globally, the agricultural sector demands approximately 70 % of global water withdrawal in numerous arid regions of the world, this demand periodically or permanently surpasses the available water resources (Hejazi et al., 2014; Seeger et al., 2016). One of the major factors responsible for aggravated water scarcity is exponentially increasing population growth and their growing needs. Consequently, leading to a substantial increase in domestic water utilization, thus generating a tremendous quantity of wastewater. It is estimated by the Indian Central Public Health and Environmental Engineering Organization (CPHEEO) that 70–80 % of the water supplied for domestic purposes emerges as wastewater (Narayan et al., 2018).

To mitigate this problem, reusing generated municipal wastewater after treatment in irrigation can be a good alternative. However, the use of inadequately treated or untreated wastewater in irrigation to agricultural fields is questionable since it embraces undesirable organics, turbidity, salinity, and most importantly, pathogenic load originating from human excreta. For unrestricted irrigation with the intention of raw consumption for crop feeding the required levels of total/faecal/thermotolerant coliforms should be <1000 colony forming units (CFU)/100 mL (United States. Environmental Protection Agency. Office of Wastewater Management. Municipal Support Division et al., 2004; World Health Organization, 2006) and at the same time, European guidelines only allow *E. coli* loads of <200 or 100 CFU/100 mL (Iglesias et al., 2010; Seeger et al., 2016). Thus, there is an imperative need for

* Corresponding author at: CSIR-Institute of Minerals and Materials Technology, Bhubaneswar, Odisha 751013, India.
E-mail address: asheesh@immt.res.in (A.K. Yadav).

https://doi.org/10.1016/j.scitotenv.2023.165320
Received 18 March 2023; Received in revised form 15 June 2023; Accepted 2 July 2023
Available online 4 July 2023

the high-quality treatment of municipal wastewater prior to reuse for agricultural purposes to achieve these stringent discharge restrictions and the safety of end users. To fulfil this purpose, low-cost technologies should be developed and opted (Saz et al., 2018; Xu et al., 2018a).

One of the conventional nature-based technologies for municipal wastewater treatment is CWs. CWs are widely adopted as secondary wastewater treatment technology and have many types; where, sub-surface flow CWs are one type of CWs that are majorly used for the treatment of domestic and municipal wastewater (Corbella et al., 2016b). Whereas, other types *i.e.*, free water surface (FWS) or floating CWs, are also widely applicable for wastewater and water bodies pollution remediation (Gupta et al., 2021a). However, high land area requirement and slow treatment limit its employment (Srivastava et al., 2019). To improve the performance of CWs, microbial electrochemical technologies (METs) such as microbial fuel cells (MFCs) are merged into CWs to form a merged technology with a name of constructed wetlands-microbial fuel cell (CW-MFC) (Yadav, 2010). Naturally occurring redox conditions in CWs facilitated a suitable environment for MFCs integration into the wetland matrix, leading to the emergence of CW-MFCs (Yang et al., 2021). CW-MFCs have also gained visibility in recent years as a promising secondary wastewater treatment technology owing to their capability of enhanced wastewater treatment with simultaneous electricity recovery as a secondary benefit (Gupta et al., 2020, 2023; Xu et al., 2018b).

The pathogen disinfection in CWs is primarily governed by vegetation and substrate, occurring either through (i) antibiotics or biocides secretion through its roots, (ii) attachment of microbes to the roots and filtration, (iii) physical processes like attachment, sedimentation, adsorption, mechanical filtration through macrophyte roots, and filter materials, killing of microbes through ultraviolet light of sun-rays, and (iv) plant and microbe interaction within the biofilm (Alufasi et al., 2017; Shingare et al., 2019). However, researchers indicated that the effluent received from CWs still records a high number of total coliform (TC), faecal coliform (FC), and *E. coli* of 4×10^6, 9×10^5, and 3×10^3 to 2×10^6 CFU/100 mL, respectively which are excessively high in comparison to discharge standard, making effluent water unsafe for reuse (Seeger et al., 2016; United States. Environmental Protection Agency. Office of Wastewater Management. Municipal Support Division et al., 2004; World Health Organization, 2006). Like other BES, some CW-MFC studies have shown the capability to produce *in situ* hydrogen peroxide (H_2O_2), which has a strong oxidizing and disinfection ability (Yang et al., 2022). The highest yield of H_2O_2 was only 2.91 mg/L in CW-MFC operated in intermittent flow conditions with filler substrate as activated carbon (Yang et al., 2022). Overall, post disinfection step of secondary effluent obtained from CWs is requisite in order to achieve the final effluent as pathogen free.

In this context, slow sand filters (SSF) could be an effective approach that has been implemented from decades for disinfection and turbidity removal in drinking water purification (Andreoli and Sabogal-Paz, 2020). Where SSF emerged as a promising technique combining both physical and biological processes for wastewater treatment. In continuous SSF, slow percolation through the filter enables physical processes like sedimentation, filtration, and adsorption, allowing retention of the large particles in the filter pore medium. At the same time, a biologically active component formed on the SSF surface with continuous wastewater flow termed as *Schmutzdecke*/dirt/hypogeal layer is responsible for most of the pathogen removal. *Schmutzdecke* layer generally consists of bacteria, protozoa, rotifer, fungi, various aquatic insect larvae, alluvial mud, zooplanktons, diatoms, and thread-like algae forms due to microbial excretion, all these facilitate pathogen removal through, elimination, natural death/inactivation, predation, mechanical trappings, adsorption, *etc.* (Andreoli and Sabogal-Paz, 2020; Bolton and Randall, 2019; Seeger et al., 2016). Overall a broad range of disinfection efficiencies has been observed through SSF for TC, FC, *E. coli*, and enterococci of 0.3–3.5 log units, 2–2.4 log units, 1.9–4.1 log units, and 0.7–3.7 log units, respectively (Kader Yettefti et al., 2013; Seeger et al., 2016). Thus, SSF could be a promising approach for the disinfection of secondary effluent with the purpose of reuse.

Accordingly, the present study investigates CW (non-conductive substrate), CW-MFC (conductive substrate), and free water surface CW (without substrate) as secondary wastewater treatment technology followed by SSF as a tertiary treatment step with the aim of enhanced treatment and disinfection of real municipal wastewater. So far, not many studies have collectively investigated different secondary wastewater treatment technologies followed by SSF in a real field setting with real wastewater treatment and addressed the following objectives. As per the author's knowledge, this study is among the first of its kind presenting main objectives as (i) evaluation of pollutant performance efficiencies of planted upscaled CW-MFCs, CWs, and FWS CWs followed by SSF for real municipal wastewater treatment, (ii) understanding how the TC, FC and *E. coli* removal efficiencies can differ with different substrates and variable *Canna indica* vegetation growth in CW-MFCs, CWs and FWS CWs, and (iii) to ensure the final effluent received after SSF treatment is safe for use in irrigation purposes.

2. Materials and methods

2.1. Fabrication of upscaled microcosms

Three upscaled CW microcosms were fabricated using linear low-density polyethylene (LLDPE) cylindrical containers of measurement 60 cm × 32.5 cm (height x diameter) and kept in natural environmental conditions in the field. All these containers were preinstalled with 3.0 sampling ports. The ports were provided from the top; the first port was at 5.5 cm followed by the middle port at 33.0 cm, and the bottom port at 57.0 cm. The top port was kept open for the entire study to ensure every microcosm maintains an equal sub-surface water level as shown in Figs. 1a and 2a. The middle and the bottom-most port for sampling and decanting the microcosms since microcosms were operated in batch mode. Three microcosms were named according to their configuration and filter substrate, such as CWs with garden gravel (CW-G), CW-MFC with granular graphite (CW-MFC-GG), and free water surface without any filter substrate (FWS-CW). Each microcosm was planted with *Canna indica* macrophyte collected from the CWs facility of CSIR-IMMT, Bhubaneswar, India. Before planting microcosms, the uprooted *Canna indica* sapling was rinsed five times using tap water. Average root length, shoot length, and weight of each *Canna indica* sapling ranged between 14.5 ± 0.5 cm, 70 ± 8 cm, and 200 ± 70 g, respectively. Each uprooted *Canna* sapling had an average of three to four leaves before transplanting to each microcosm as shown in Fig. 2b. While fabricating the microcosms, large gravels with an average diameter of 20.0–25.0 mm were added to each microcosm up to the height of 10.0 cm from the bottom as a supporting layer except for FWS-CWs system in which large gravels layer was up to 14.0 cm to hold a polyvinyle chloride (PVC) pipe of Ø (diameter 20.0 mm) situated in center for supporting the *Canna indica* plant, as shown in Fig. 1c. In each microcosm a PVC pipe (Ø = 20.0 mm) was fitted in the center to serve multiple purposes such as gas vent, water level measurement (evapotranspiration) and supporting the plants for the case of FWS-CW.

On the top of large gravels, CW-G was filled with small size gravels (Ø = 5.0–8.0 mm). *Canna indica* plants were planted in all the microcosms. The fabrication of CW-MFC-GG (Fig. 1a) differed from CW-G (Fig. 1b). In CW-MFC-GG, after the lining of a 10.0 cm layer of large gravels, it was overlaid by a 15.0 cm layer of granular graphite (Ø = 5–8 mm) for working as an anode, in this layer, a graphite plate of 400.55 cm^2 surface area was also inserted to work as electron collector. Thereafter, a 20 cm layer of normal gravel (Ø = 5–8 mm) was used as a separator enclosed by a double lining of high-density polyethylene (HDPE) liner (with some holes for water percolation) at both ends, further overlaid by 15.0 cm of granular graphite layer for working as a cathodic layer. In the cathodic layer, a graphite plate was inserted to work as an electron dispenser (400.55 cm^2 area) was kept. The anode

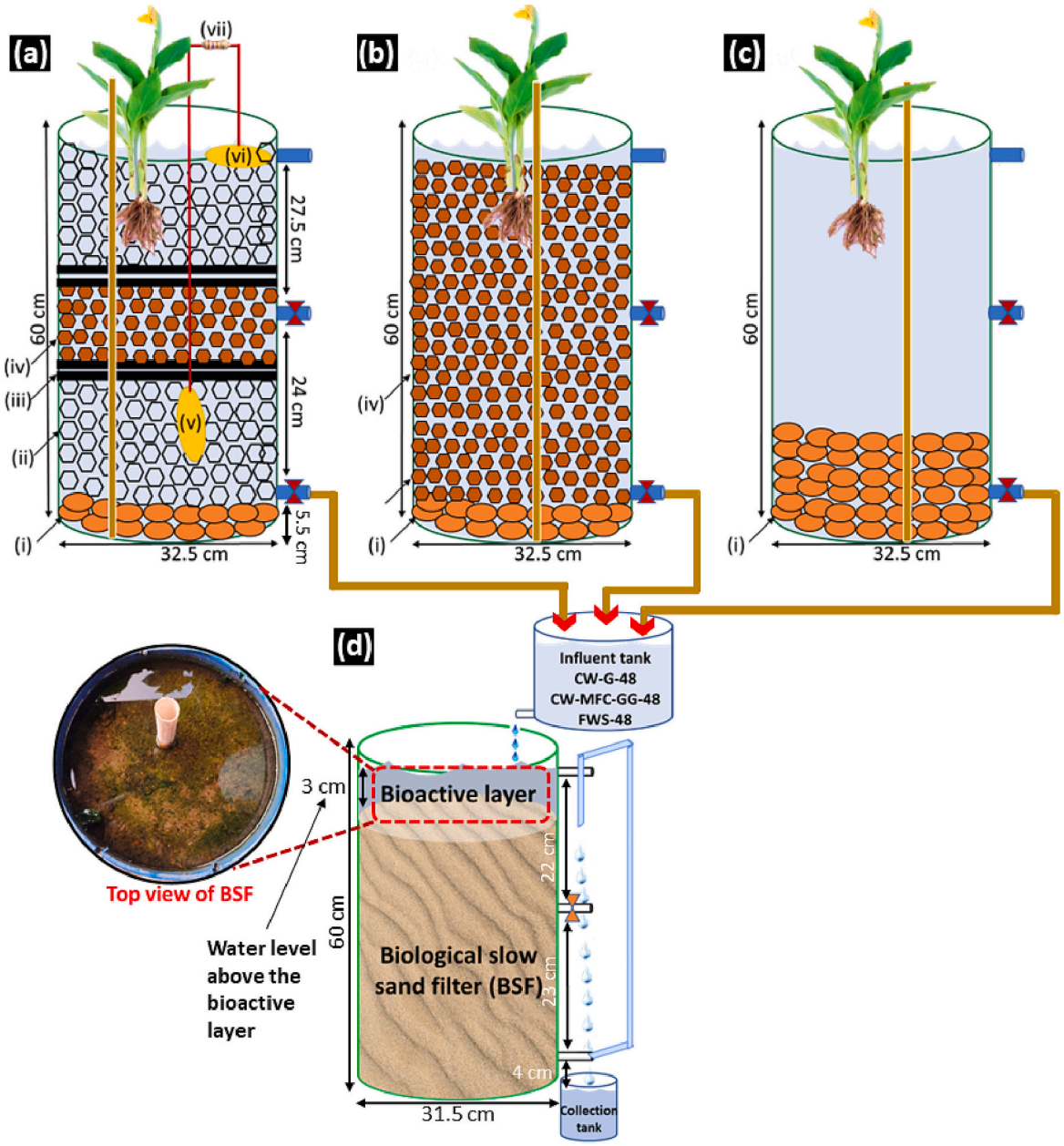

Fig. 1. Schematic view of (a) constructed wetlands *cum* microbial fuel cell with granular graphite (CW-MFC-GG), (b) constructed wetlands with gravel (CW-G), (c) free water surface-constructed wetlands (FWS-CW), and (d) slow sand filter (SSF) with an enlarged view of its top bioactive (schmutzdecke) layer. In Fig. 1, (i) represents a boulder of average size 20–25 mm; (ii) is the anodic layer of granular graphite (5–8 mm Ø); (iii) double layered high density polyethylene liner (HPDE); (iv) gravel (5–8 mm Ø) separation; (v) anode charge collector/dispenser; (vi) cathode charge collector/dispenser, and (vii) resistance load connected between anode and cathode.

and cathode charge collector/dispenser were connected with insulated copper wire and the exposed area was sealed and insulated with epoxy. The other free ends of the anode and cathode charge collectors/dispenser were connected with a resistance (as shown in Fig. 1a)

2.2. Slow sand filter assembly

SSF with a bed depth of 60 cm was constructed in an LLDPE container of 60 cm height and 31.5 cm diameter and equipped with 3 ports at a distance of 4 cm, 27 cm, and 49 cm from the bottom, as shown in Fig. 1d. In the SSF unit, a 3.0 cm deep bed of large gravels (Ø = 20–25 mm) followed by a 3 cm deep bed of garden gravel (Ø = 5–8 mm) was placed in the bottom section. The rest of the space in the SSF unit was filled with river sand. The river sand used in SSF was having effective size *i.e.*, D_{10} (average particle diameter in mm) and $\frac{D_{60}}{D_{10}}$ uniformity coefficient (grain size distribution) as 0.240 mm and 2.70 mm, respectively. Further, fabricated SSF was continuously monitored and operated in continuous mode for 2 months with the final effluent of CSIR-IMMT CW facility for acclimatization of schmutzdecke layer. SSF was fed with 48 h treated effluent from CW-G, CW-MFC-GG, and FWS CWs microcosms. SSF was operated in continuous mode through drop-wise wastewater distribution from the reservoir tank (30 cm height, Ø = 15 cm) outfitted with a tap. To maintain the average flow rate of 116 mL/h it was ensured that the reservoir was always filled >75 % of its capacity. Since SSFs operate in down flow motion, the effluent pipe was siphoned from the bottom port to maintain the water level above the top active schmutzdecke layer (promotes pathogen removal), and the effluent pipe was further curved over the top port permitting the

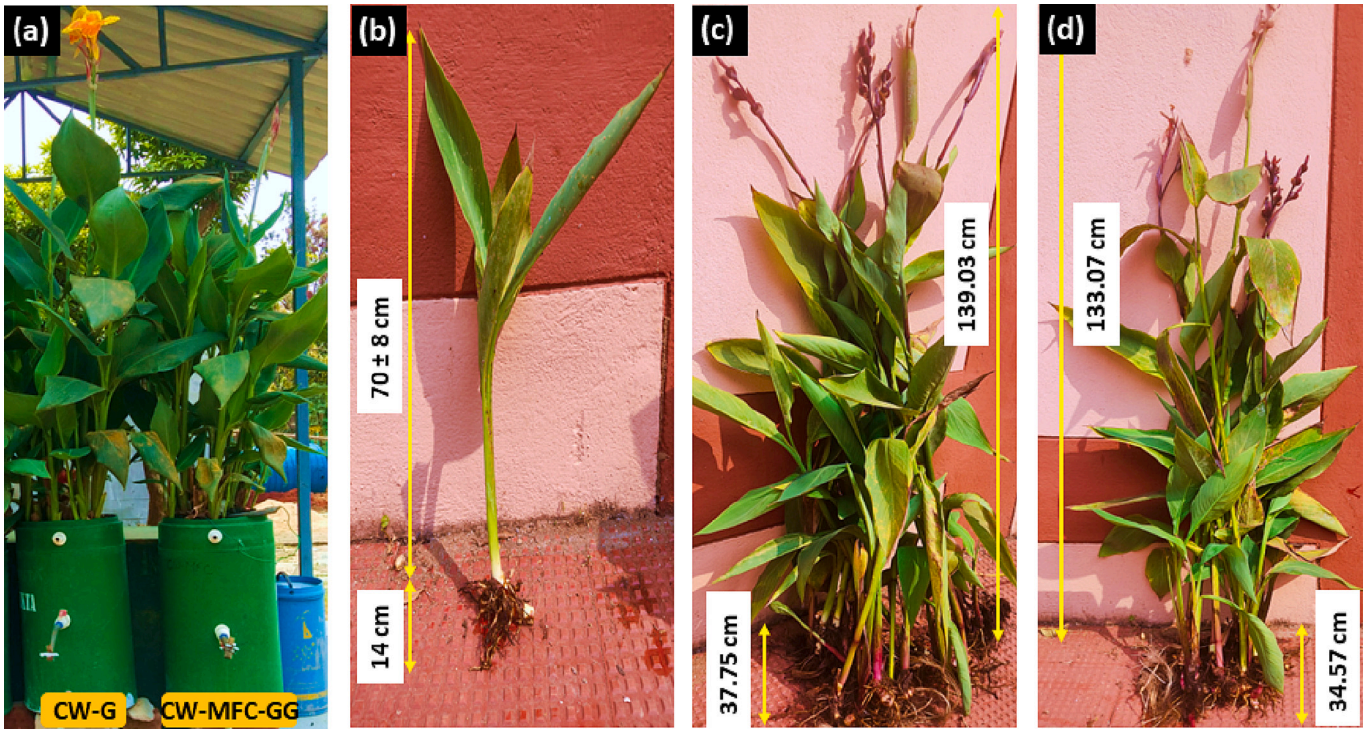

Fig. 2. (a) Real field pictures of CW-G and CW-MFC-GG microcosms (b) Representative initially planted *Canna indica* saplings, (c) and (d) Representative harvested plant biomass from CW and CW-MFC microcosms, respectively.

discharge through gravity, as shown in Fig. 1d. Thus, siphoning of effluent pipe enabled the maintenance of water level up to 3 cm above the top active schmutzdecke layer (Fig. 1d). The SSF unit was used for each microcosm's effluent for a study duration of 45 days. Effluent of a microcosm was fed to SSF then after a retention time of 48 h SSF effluent was collected. Similarly, the same procedure was repeated for other disinfection experiment with the 48 h effluent of other microcosms. The collected samples from the SSF were further analyzed for assessing the treatment performance and disinfection. Analyzed parameters were turbidity, chemical oxygen demand (COD), phosphate, total coliform (TC), faecal coliform (FC), and *E. coli*.

2.3. Experimental operation and sample collection

During the experiment, real municipal wastewater, after primary treatment, was fed to the microcosms from the CW facility situated on-campus at CSIR-IMMT, Bhubaneswar, India. During the acclimatization phase of nearly two months, microcosms were fed in a 1:1 ratio of new wastewater and effluent from the microcosms. Acclimatization of microcosms was considered on parameters such as the development of *Canna indica* vegetation, the stable voltage output by CW-MFC-GG, and consistency in pollutant removal efficiencies of microcosms. After the completion of the acclimatization phase, microcosms were considered ready for further studies.

At first, 80 liters (L) of real municipal wastewater was stored in a PVC tank to maintain and mixed well to feed homogenous wastewater into the microcosms; approximately 50 mL was collected as influent wastewater in a sample bottle from the tank. After that, wastewater was fed through the top of each microcosm by slowly percolating the wastewater from the top; the initial working volume for each microcosm was measured as: 16.75 L (CW-G), 18.5 L (CW-MFC-GG) and 33 L (FWS). This hour (h) of microcosm filling was considered as 0 h of batch loading, here onwards each microcosm was gone through the entire following procedure at each 8 h, 24 h, and 48 h: (i) each microcosm was entirely decanted, (ii) decanted wastewater was homogeneously mixed for sample collection (volume collected: 50 mL), (iii) decanted volume was measured for evaluation of evapotranspiration (ET) through each microcosm and (iv) refilled again with the same decanted wastewater. This entire cycle of 48 h was carried out once a week after the rainy season's end and continued for 6 months from September 2020 to February 2021. Further, collected samples were kept at 4 °C and analyzed on the second day of sample collection for COD and phosphate.

2.4. Most probable number (MPN) for the enumeration and quantification of bacteria

MPN was conducted in three steps, namely presumptive test, confirmatory test, and complete test for the determination of total coliform (TC), faecal coliform (FC), and presence/absence of *E. coli* in the wastewater samples. MPN was conducted with influent samples and was compared with effluent samples collected after treatment from each CW microcosm and their respective collected SSF effluent.

In the presumption test, three sets of sterilized test tubes were prepared; each set contained five test tubes with an inverted Durham tube. Each tube was prepared with 10 mL of broth, whereas one set contained double-strength MacConkey broth while the other two sets contained neutral-strength MacConkey broth and were inoculated with 10, 1, and 0.1 mL of 48 h treated wastewater samples of each microcosm and further SSF treated samples of each microcosm, respectively. Afterward, all the test tubes were incubated at 37 °C for 24–48 h. After incubation for 24 h, each test tube was examined for gas production (coliform bacteria produce gas from the lactose which was trapped in the inverted Durham tube) (ISI, 1982). The positive tubes with gas production were counted, and MPN determination was carried out through a standard chart in terms of coliform forming units per 100 mL (CFU/100 mL) of wastewater sample as carried out by other researchers (Ajonina et al., 2015; Torrens et al., 2009).

Further, the confirmatory test was carried out for faecal coliform in brilliant green bile lactose broth medium (BGLB). For that 100 μL of positive samples from the presumptive test were taken and inoculated in BGLB broth. Two sets of BGLB tests were prepared containing inverted Durham tubes, where one of the sets was incubated at 37 °C and the

other one at 44 °C for 24–48 h.

Thereafter for the *E. coli* confirmation test, 100 μL of subculture from positive tubes of the confirmatory test was inoculated into peptone water broth and incubated at 44.5 °C for 24 h. At the end of the incubation period, a test for indole production by adding a few drops of Kovac's reagent was performed (ISI, 1982). Further, the percentage removal of CFU units was also carried out with the obtained data through Equation (Eq.) (1), where the number of viable microorganisms before treatment is represented by V_{before}, and the number of viable microorganisms after treatment is represented by V_{after}:

$$\%removal = \frac{V_{before} - V_{after}}{V_{before}} \times 100 \quad (1)$$

2.5. Analysis for pollutant assimilation in plant biomass

After six months of experimental operation, biomass was harvested completely (along with root) from all the microcosms. The root length, shoot length and weight of harvested biomass were measured and noted for comparison with the initial *Canna indica* planted sapling. Each plant biomass collected from the microcosms was further separated out as leaves, stems, and roots and dried at 80 °C until a constant weight was recorded on weighing at frequent intervals. The dried biomass was ground to powder and collected separately as roots, stems, and leaves. Later, 0.5 g of each collected sample was digested in a 50 mL mixture of $HClO_4$ and HNO_3 (1:1 ratio) at 100 °C in a fume hood (SS Godrej fume hood, India) till residual digestion acid mixture became 2 % of the initial mixture (*i.e.*, 1 mL). Further, each sample was filtered out (0.45 μ pore size Whatman filter paper), and filter paper was thoroughly rinsed with distilled water to make volume up to 100 mL in a volumetric flask (Du et al., 2018). After that phosphate analysis was carried out. Further, assimilation in plants has been expressed in mg/g and calculated with the Eq. (2):

$$PO_4^{3-}(mg/g) = \frac{PO_4^{3-}(mg/L) \times 0.1\ (volume\ factor\ in\ L) \times dilution\ factor}{0.5\ (dry\ weight\ of\ sample\ in\ g)} \quad (2)$$

2.6. Wastewater analysis

All samples were analyzed for (COD) and phosphate as described in standard methods of American Public Health Association (APHA) as 5220D-Closed Reflux, Colorimetric Method, and 4500-P D stannous chloride method, respectively (American Public Health Association, 2005). All samples were filtered out using 0.45 μ pore size Whatman filter paper. The final pollutant treatment efficiency (%) after considering ET was calculated by entering the received pollutants effluent concentration in Eq. (3) followed by Eq. (4) and Eq. (5):

$$Loss\ of\ water\ volume\ (\%) = \frac{Influent\ volume\ (L) - Effluent\ volume\ (L)}{Influent\ volume\ (L)} \times 100 \quad (3)$$

Effluent pollutant concentration after removing water loss (%) (Q) in mg/L was calculated by Eq. (4).

$$Q(mg/L) = Effluent\ pollutant\ concentration\left(\frac{mg}{L}\right) \times \left(1 - \frac{loss\ of\ water\ volume\ (\%)}{100}\right) \quad (4)$$

Further, the total percentage removal efficiency (RE) of the pollutant after considering ET was calculated by Eq. (5)

$$RE(\%) = \frac{Influent\ pollutant\ concentration\ \left(\frac{mg}{L}\right) - Q\ \left(\frac{mg}{L}\right)}{Influent\ pollutant\ concentration\left(\frac{mg}{L}\right)} \quad (5)$$

Influent was also analyzed for biological oxygen demand (BOD) as described by other researchers (Samantray et al., 2009).

In addition, percentage (%) volume reduction was calculated based on the volume at the start of the experiment ($Volume_{start}$) and reduction in the working volume of microcosms at the end of the experiment ($Volume_{end}$) by Eq. (6):

$$\%volume_{reduction} = \frac{Volume_{start}(L) - Volume_{end}(L)}{Volume_{start}(L)} \times 100 \quad (6)$$

The dissolved oxygen (DO) of the top, middle and lower region of each microcosm was measured with DO probe, HACH HQ-40D (USA), while the pH was measured using a pH meter (Eutech instruments cyberscan pH 1500, Canada). Furthermore, the turbidity of samples was measured by turbidimeter (2100P, HACH, USA).

In the case of CW-MFC-GG, voltage generation was recorded on a daily basis with a digital handheld multimeter (Fluke 17B, USA). The polarization experiment was performed at variable external resistances (10 K Ω–100 Ω) under closed circuit conditions to obtain current and power. Internal resistance was determined through a polarization curve plot between current density (mA m^{-3}), power density (mW m^{-3}), and attained voltage (V). Current density and power density were calculated by dividing generated current and power by the anodic volume (m^3) of CW-MFC-GG.

3. Results and discussion

3.1. Macrophytes growth assessment

After the transplantation of macrophytes into each microcosm, it exhibits healthy growth throughout the experimental period with the flourished root system. At the end of the study, root length increased from 14 cm to 37.75 cm and 34.57 cm for CW-G and CW-MFC-GG, respectively, as shown in Fig. 2b, c, and d. The shoot length increased from 70 ± 8 cm to 139.03 cm and 133.07 cm for CW-G and CW-MFC-GG, respectively. The grown root and shoot length indicated the macrophytes had proper growth conditions to reproduce well in the microcosms. However, macrophytes in the FWS microcosm could not flourish well due to the unavailability of substrates to hold the vegetation. A similar increase in root and shoot has also been observed with different types of vegetation such as *Typha angustifolia*, *Juncus gerardii*, *Carex divisa* (Saz et al., 2018), *Iris pseudacorus*, and *Phragmites australis* (Yang et al., 2020) in CW and CW-MFC microcosms. After harvesting the macrophytes from the microcosms, a total wet weight of 4.254 kg and 4.628 kg was observed for CW-MFC-GG and CW-G, respectively. The total dry biomass computed was 48.89 kg/m^2 for CW-MFC-GG. Whereas CW-G exhibited total dry biomass of 50.313 kg/m^2. A slight difference in total dry biomass of CW-MFC-GG and CW-G may be due to the positioning of the HDPE liner (double plastic layer) in CW-MFC-GG. It was placed just beneath the macrophytes to avoid the cross-over of roots to the anodic region of CW-MFC-GG. This may have restricted roots from growing further and thus moderately reducing the overall dry biomass of CW-MFC-GG compared to CW-G. Further, total working volume reduction in microcosms was calculated from the start of the experiment (planting a plant sapling) to the end of the experiment (fully flowered *Canna indica* plant growth). The volume reduction was observed highest for CW-G *i.e.*, 16.41 % followed by CW-MFC-GG (10.81 %), and FWS of 4.69 %. One associated phenomenon with volume reduction is the amount of sludge generation (Srivastava et al., 2021a, 2021b). Accumulation of organic/inorganic substances in sludge can ultimately lead to clogging, resulting in a decreased life span of the system in the long term. Clogging can further complicate the pollutants removal in the system and hinder the system's treatment performance (Corbella et al., 2016a). Among substrate-based microcosms, *i.e.*, CW-G and CW-MFC-GG, the highest volume reduction was observed in CW-G; this signifies that CW-G will earlier reach the clogging stage with reduced treatment performance compared to CW-MFC-GG. Similar results are also revealed by Srivastava et al. (2021a), where a high volume reduction of 1.3 L was observed in CW compared to 0.5 L in CW-MFC. Besides, the reason for

the lowest volume reduction in FWS resulted from its design and configuration *i.e.*, without substrate. The maximum volume reduction in CW-G was also in agreement with overall biomass generation *i.e.*, the highest in CW-G. This signifies a more significant consumption of void spaces in CW-G by the root expansion with time, leading to the maximum reduction in microcosm volume. The difference in root growth and biomass can also cause variations in the disinfection efficiency, pollutant removal performance of different microcosms, and electricity generation in the case of CW-MFC-GG (Yang et al., 2021).

3.2. Disinfection and turbidity removal assessment

MPN technique was employed for the enumeration and quantification of TC, FC, and *E. coli* bacteria. The reduction in TC and FC was observed at 48 h in treated effluent of CW-G, CW-MFC-GG, and FWS, as shown in Fig. 3. Gas formation within the incubation period at 44 °C was considered a positive reaction for FC, whereas gas formation at 37 °C provided TC. The maximum reduction of TC was observed in CW-G, and the minimum was for FWS microcosm effluent, on the other hand, FC was removed by 55.71 % in both CW-G and CW-MFC-GG and minimally removed in FWS (Fig. 3a and b). Further, 48 h treated wastewater from CW-G, CW-MFC-GG, and FWS were fed to SSF having a retention time of 48 h. SSF presented 50.57 % and 100 % reduction in TC and FC, respectively from CW-G effluent and 68.26 % and 100 %, respectively from CW-MFC effluent, shown in Fig. 3a and b. The presence and absence of faecal coliform *E. coli* from the effluent of all microcosms were also evaluated and found to be absent/negative in the SSF effluents where effluents of CW-G and CW-MFC-GG were fed as influents. In contrast, it was positive in SSF effluent where effluent of FWS was used as an influent (Fig. 3c). This indicated even after 48 h of treatment through FWS-SSF coupled system, the faecal coliform *E. coli* number was high. The high pathogen removal from SSF was mainly due to a slow filtration rate of 0.10 cm h^{-1}, which allowed longer retention and competitive interaction of pathogens with other organisms in the microcosms. Similarly, in another study by Tyagi et al. (2009), SSF was also found promising as a post treatment technique for upflow anaerobic sludge blanket microcosm effluent, reporting significant removal of 99.95 % of TC and FC in SSF effluent at a filtration rate of 0.14 m/h. In SSF, the schmutzdecke layer has played a crucial role in biological pathogen removal mechanisms. This layer slowly forms over the top of fine sand particles due to the establishment of a microbial and algal community. In this majority of the microbial population are predatory bacteria which feed upon the water-borne microbes passing through the filter (Ranjan and Prem, 2018). It may include predation by eukaryotic bacterivores (such as heterotrophic non-flagellates and protozoa), and by *Bdellovibrio* species together with lysis stimulated by bacteriophages. The other involved mechanism in SSF for TC, FC, and *E. coli* removal are: (i) straining, (ii) adsorption, (iii) natural die off in non-biological sand filter zone due to starvation, and (iv) algal derived reactive oxygen species (Seeger et al., 2016). Whereas, the role of macrophytes is also being reported for pathogen removal by secreting antibiotics or biocides through their roots (Shingare et al., 2019); perhaps similar reasons may also be active in our studies. In CW-MFC-GG, slightly low removal of total coliform may be due to the fact that roots of *Canna indica* could not cross over to lower anodic region and since microcosms were operated in batch mode, wastewater could not sufficiently circulate inside the microcosms. In addition, a persistently low BOD/COD ratio indicates complex wastewater with low biodegradability, which leads to a decrease in the functioning of electroactive microbes for degradation of non-biodegradable matter in CW-MFCs (Deval et al., 2017; Liu et al., 2014). The planted CWs have been reported by several studies for enteric pathogen removal, such as *Coliform*, *Shigella*, *Salmonella*, *Coliphage*, and *Enterococcus* (Shingare et al., 2019). For instance, a reduction of *E. coli* by 2.58 log and TC by 0.82 log was observed in pilot scale horizontal surface flow CW planted with *Canna indica*, and further reduction of TC by 1.55 log was achieved in followed vertical flow CW also planted with *Canna indica* (Zurita and Carreón-Álvarez, 2015). FWS has less reduction of TC and FC since *Canna indica* could not flourish

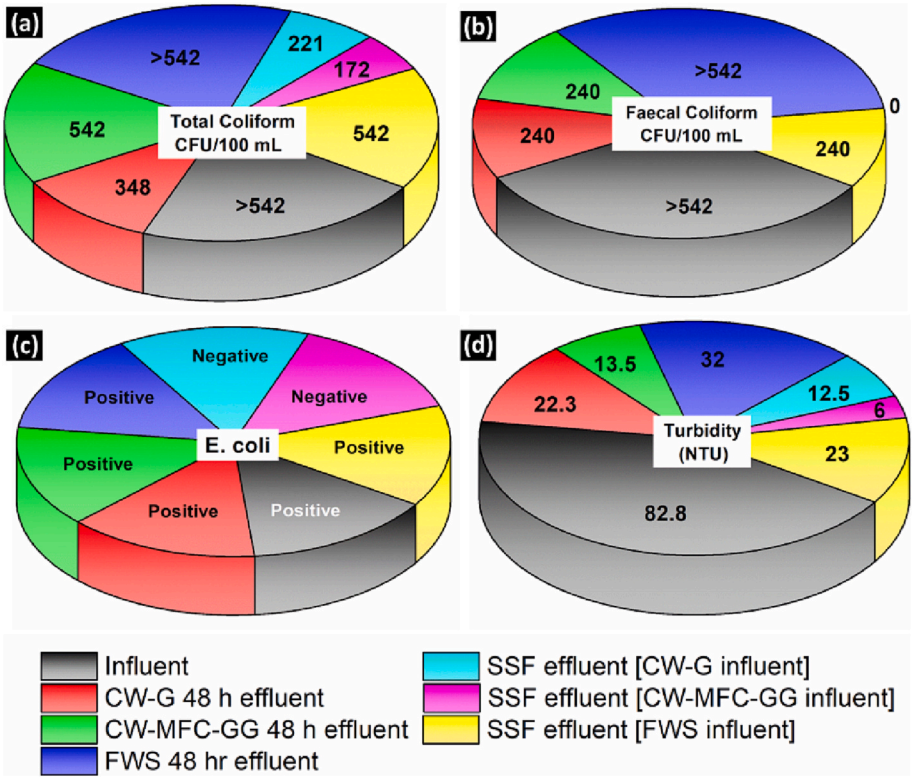

Fig. 3. (a) Total coliform removal (CFU/100 mL), (b) Faecal coliform removal (CFU/100 mL), (c) *E. coli* coliform, and (d) Turbidity in NTU, for influent, CW-G, CW-MFC-GG, FWS at 48 h and after treatment through SSF.

properly in the system and limited biological activity as lesser microbial biofilm formation due to non-availability of filter materials.

Furthermore, microbiological variables (TC, FC, and *E. coli*) are also directly correlated with the physicochemical parameter for example turbidity. Tyagi et al. (2009), revealed that reduction in all types of microbiological variables is related to physicochemical parameters with a correlation coefficient of 0.91 to 0.97. Both physicochemical and microbiological parameters follow the same downward trend and were driven by the common force *i.e.*, the straining and attachment pattern to medium/filter material/substrate for removal of pollutants are almost similar to the straining and attachment pattern followed by biofilm growth and predator capturing in Schmutzdecke layer (Tyagi et al., 2009; Weber-Shirk and Dick, 1997). In the present study, the wastewater fed to the microcosms had high levels of turbidity.

The turbidity of 82.8 NTU was observed in influent wastewater, which significantly decreased in 48 h of retention time to 22.3 NTU, 13.5 NTU, and 32 NTU for CW-G, CW-MFC-GG, and FWS, respectively, as shown in Fig. 3d. The highest decrease in turbidity was noted in CW-MFC-GG and lowest in FWS, which could be due to the microcosm's filter materials (porous graphite granules) that acted as a better filter. However, the absence of filter materials in the FWS microcosm could be the reason for minimal turbidity removal (Fig. 3d). Zhao et al. (2013) also reported higher turbidity removal efficiency in batch-operated CW-MFC. Moreover, high root biomass in CW-G and CW-MFC-GG also played an important role in trapping suspended particles, resulting in high turbidity removal. Generally, 10 to 50 NTU is recommended to be treated in the slow sand filters to avoid clogging and proper functioning of slow sand filters (CAWST, 2012). In this study, the obtained turbidity after 48 h treatment through microcosms was within the recommended range to be treated by SSF. The microcosms effluents were further passed through SSF, where a considerable decrement of turbidity 43.9 % (12.5 NTU), 55.55 % (6 NTU), and 28.12 % (23 NTU) was observed for CW-G, CW-MFC-GG, and FWS effluent, respectively as shown in Fig. 3d. The obtained results are in agreement with other studies, where traditional household SSF and compact household SSF has reduced the turbidity from 13.2 ± 14.6 NTU to 3.13 ± 4.77 NTU, and 3.30 ± 5.24 NTU, respectively (Freitas et al., 2021). The high turbidity removal efficiencies through SSF could be owing to stable Schmutzdecke development *via* constant and low filtration rates in SSF (Andreoli and Sabogal-Paz, 2020). Altogether, turbidity removal through CW-MFC-GG-SSF outperformed CW-G-SSF and FWS-SSF with obtained removal efficiencies of 92.75 %, 84.90 %, and 72.22 %, respectively. Decisively, tertiary treatment through SSF in combination with secondary treatment through CW-MFC-GG could be a promising approach towards disinfection along with turbidity removal.

3.3. Treatment performance assessment

3.3.1. COD removal

The upper, middle and lower DO profile and pH profiles of CW-G, CW-MFC-GG and FWS were also measured. However, upper DO and pH of CW-G and CW-MFC-GG could not be measured due to the unavailability of water samples on the upper surface owing to high ET through the systems (Fig. 5d). This further allows high diffusion of atmospheric oxygen inside the upper region of CW-G and CW-MFC-GG. Although, middle and lower regions seems to be mostly anaerobic by nature for CW-G and CW-MFC-GG with DO levels 1.21 ± 1.35 mg/L, 1.35 ± 0.75 mg/L in CW-G; 1.27 ± 0.89 mg/L, 1.12 ± 0.35 mg/L in CW-MFC-GG respectively. Although, attained DO range in the anode of CW-MFC-GG was suitable for the functioning of electroactive bacteria (EABs) (Mittal et al., 2022). FWS showed upper, middle, and lower DO levels of 1.12 ± 0.43 mg/L, 0.92 ± 0.45 mg/L, and 0.98 ± 0.88 mg/L respectively indicating low DO in all regions with an insignificant difference in DO values of different regions. Similar results were also observed in the winter season by He et al. (2012), where DO vary in the range of 0.37 ± 0.28 mg/L to 0.91 ± 0.28 mg/L in FWS systems. Furthermore, pH values were measured as 6.3 ± 0.15, 6.27 ± 0.22 in CW-G; 6.33 ± 0.17, 6.31 ± 0.12 in CW-MFC-GG in the middle and lower region, respectively, whereas in the case of FWS, it was 6.62 ± 0.10, 6.57 ± 0.16, 6.47 ± 0.18 in upper, middle, and lower regions, respectively. The insignificant difference in pH values in different regions of all microcosms signifies high buffering capacity and efficient growth of microbes throughout systems (Mittal et al., 2023b; Saket et al., 2021; Saeed et al., 2022).

The treatment assessment of the microcosms was observed based on COD removal performance. The influent COD concentration of wastewater varied between 25.63 mg/L to 327.41 mg/L with 125.35 ± 77.93 mg/L average influent concentration. However, influent wastewater showed low BOD resulting in a very low BOD/COD ratio of 0.0005, indicating the highly recalcitrant nature of municipal wastewater with low biodegradability. The COD removal of all microcosms at 8 h, 24 h, and 48 h have been displayed in Fig. 4a, b, and c. The average COD percentage removal in 8 h, 24 h, and 48 h for CW-G was 38 ± 22 %, 46 ± 28 %, and 63 ± 20 %, respectively, likewise in CW-MFC-GG it was 33 ± 22 %, 48 ± 23 %, 57 ± 24 %, and in FWS, it was 12 ± 13 %, 28 ± 12 %, and 30 ± 20 %, respectively. The high variation in COD removal throughout the study was due to fluctuation in initial COD concentration from low to high. That fluctuation could have affected the overall microbiology of the microcosms. Further, in Fig. 4a, b, and c, an increase in overall COD removal with an increase in HRT was also observed, where, in 48 h slightly higher average removal was observed in CW-G compared to CW-MFC-GG. Similar results were also observed in a recently published study by Yang et al. (2022) while treating pond water containing a low initial COD concentration of 132 mg/L with CW-MFC and CW pilot scale microcosms. The study reported that the effluent COD concentration of CW-G and CW-MFC were 30 mg/L and 44 mg/L, respectively, the reason behind high COD removal in CW microcosm compared to CW-MFC was reported as low influent COD concentration, which restricted the exertion of CW-MFC advantages (Yang et al., 2022). Moreover, in the present study, a very low BOD/COD ratio shows the complexity of wastewater that created complexity for electrogenic microorganisms existing in CW-MFC-GG to extract energy from such wastewater and thus limiting the COD removal in CW-MFC-GG (Deval et al., 2017; Liu et al., 2014). Furthermore, the difference in void volume can also play a significant role in COD removal. Lower the void volume higher will be the loading rate of pollutants, thus, allowing different loading rates. This could be one of the reasons for slightly low COD removal in CW-MFC-GG compared to CW-G since the void volume of CW-G is higher than CW-MFC-GG; thus, the COD loading rate is higher in CW-MFC-GG. These results are in agreement with the studies demonstrating decreasing trend in the removal efficiency with an increase in pollutant loading rate (Ávila et al., 2014; Tamta et al., 2023; Yang et al., 2016). This also explains the reason for the lowest COD removal in FWS since it had twice the void volume, thus twice the loading rate than CW-G and CW-MFC-GG.

3.3.2. Phosphate removal

The performance of all microcosms was also assessed based on phosphate removal. The influent phosphate concentration varied between 0.87 mg/L to 9.68 mg/L with 5.12 ± 2.43 as the average influent concentration. The average phosphate removal at 48 h HRT from CW-G, CW-MFC-GG, and FWS was 91 ± 7 %, 84 ± 11 %, and 31 ± 19 %, respectively, as shown in Fig. 5a, b and c. The higher phosphate removal in CW-G and CW-MFC-GG could be due to high plant biomass which increased adsorption and accumulation of phosphate in the plant tissues (Saz et al., 2018). Results indicated maximum phosphate assimilation of 0.52 mg/g and 0.51 mg/g in the stem of CW-G and CW-MFC-GG, respectively, as shown in Fig. 5e. There are other studies which also reports similar phosphate uptake by different plant species such as Li et al. (2013) found 0.89–2.18 mg/g total phosphorous uptake by six different vegetation in CW, including *Canna indica* whereas 1.4 mg/g of phosphorous uptake was observed by Zhang et al. (2009) by *Canna*

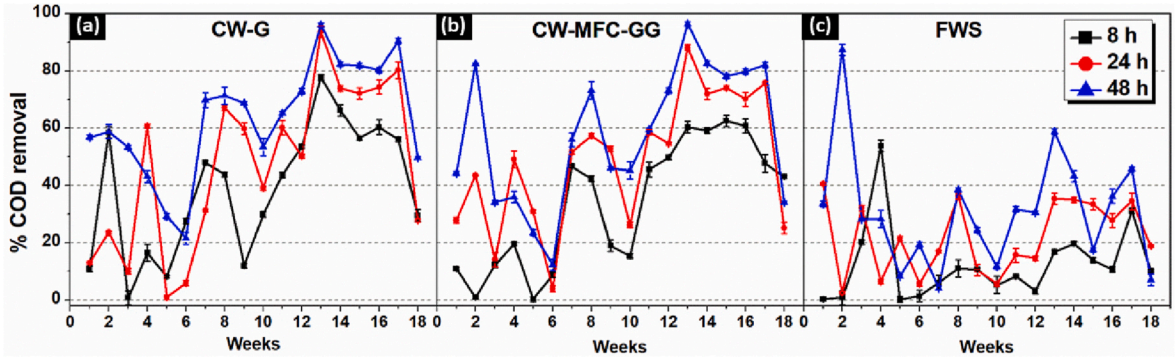

Fig. 4. COD removal by (a) CW-G, (b) CW-MFC-GG, and (c) FWS microcosm at 8 h, 24 h and 48 h.

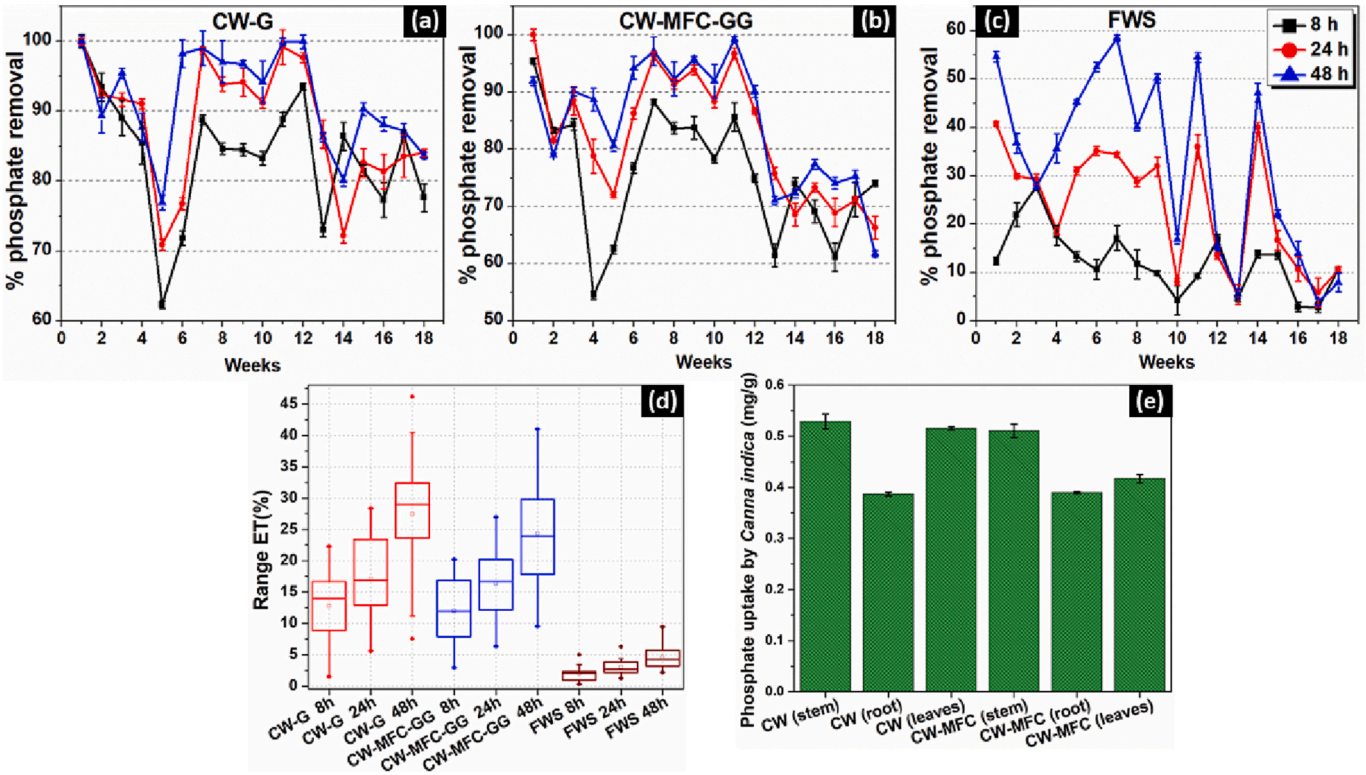

Fig. 5. Phosphate removal by (a) CW-G, (b) CW-MFC-GG, and (c) FWS microcosms, (d) Range of ET, and (e) phosphate uptake by root, stem, and leaves of *Canna indica* vegetation in CW-G and CW-MFC-GG.

indica from simulated secondary treated wastewater. This suggests that assimilation in vegetation played significant role in phosphate removal. The results similar to the present study are also reported by Yang et al. (2022) while treating pond water with a very low total phosphorous concentration of 0.34 mg/L. This study by Yang et al. (2022) reported that at the end of 56 days of stable operation, total phosphorous concentration in CW-MFC effluent was found to be higher than CW effluent *i.e.*, 0.029 and 0.014, respectively.

It is very well known that phosphate removal is primarily governed by filtration media. The efficiency of filtration is closely related to the physical and chemical properties of filter media such as specific surface area, size, porosity, and adsorption (Mu et al., 2021). Both gravel and granular graphite filter material had almost similar sizes; however, granular graphite particles are comparatively coarser than gravel particles. Along with this, granular graphite is also conducive to the diffusion of pollutants due to its high surface area and its porous structure (Taskan and Hasar, 2015; Zhou et al., 2011). But at the same time, granular graphite only contains inert fixed carbon material and along with this graphite is a more structured material so it may be less interactive than normal gravel, allowing differences in adsorption properties of gravel and graphite and the reason for lesser adsorption capacity in granular graphite. The extracellular polymeric substances (EPS) in the biofilm formed over the surface of gravel and granular graphite can also contribute to phosphorous removal through adsorption (Xu et al., 2019; Zhao et al., 2020).

Furthermore, extensive root systems in both CW-G and CW-MFC-GG played a crucial role in phosphate removal through adsorption. The slightly high phosphorous removal in CW-G compared to CW-MFC-GG could be due to a more extensive root system due to the higher biomass of CW-G compared to CW-MFC-GG. Whereas lowest phosphate removal in FWS was due to the unavailability of the substrate and non-flourished *Canna indica* vegetation.

The high ET in CW-G and CW-MFC-GG (as shown in Fig. 5d) allows the formation of large air exposed upper portion, which may have provided favorable conditions for the functioning of phosphorous-accumulating organisms (PAOs) in both microcosms for phosphate

removal. However, a similar could not apply in the case of FWS since *Canna indica* vegetation could not flourish in the system, and very low ET was computed which was mainly due to evaporation.

3.4. Treatment performance of slow sand filter (SSF)

SSF was employed as tertiary treatment technology with the primary purpose of disinfecting the secondary effluent received from CW-G, CW-MFC-GG, and FWS microcosms. Simultaneously, it was also investigated for pollutant removal efficiency, where COD and phosphate concentration before and after the slow sand filter is represented in Fig. 6. The COD removal observed in SSF was not significant due to very low residual COD concentration caused by residual recalcitrant pollutants after treatment through CW-G and CW-MFC-GG. However, the residual COD concentration after treatment through FWS was higher, and thereby removal of 19.08 % was observed, decreasing the average COD concentration from 59.92 ± 2.04 mg/L to 48.49 ± 1.48 mg/L, as shown in Fig. 6. These results are in agreement with other studies reporting less organic matter removal in slow sand filters at low influent COD concentration (Verma et al., 2017). Generally, COD is utilized by the microbial population present in schmutzdecke layer, and limited COD availability could restrain the development of the microbial community. As a result, microorganism growth is often accompanied by a dying-off process, releasing organic matter that is then accessible to bacteria up to some depths. These bacteria utilize some part of it as food to gain the energy required for their metabolism and other parts for their cell material and their growth. In this way, the dead matter generates live matter again allowing survival and sustenance of schmutzdecke layer microbial community even at low influent COD concentration (Ranjan and Prem, 2018).

Furthermore, some reduction in the concentration of phosphate was observed in SSF after treatment through all the microcosms, as shown in Fig. 6. The phosphate removal of 85 % ± 0.05, 76.63 ± 0.01 % and 43.45 ± 0.2 % was observed through SSF, attaining phosphate concentration in the effluent as 0.42 ± 0.002 mg/L, 0.68 ± 0.005 mg/L and 2.03 ± 0.02 mg/L for CW-G-SSF, CW-MFC-GG-SSF, and FWS-SSF, respectively. The observed removal could be through the formed gelatinous layer/schmutzdecke layer (Seeger et al., 2016). In SSF, the top zone of the reddish-brown sticky film was observed. It is mentioned in several studies that this reddish-brown sticky film also contains thread-like algae developed by microorganism excretion (Verma et al., 2017). This thread-like algae present in the schmutzdecke layer is generally responsible for utilizing phosphate for their growth and metabolism along with passive aeration (Gupta et al., 2021b). Furthermore, since in SSF, wastewater slowly percolates in a downward motion through the sand column, increasing the contact time between wastewater and schmutzdecke layer and resulting in higher phosphate removal (Seeger et al., 2016). In summary, the effluent concentration of phosphate and COD by CW-G-SSF and CW-MFC-GG-SSF have fulfilled the standard discharge limits as set by the Environmental Protection Agency (EPA) (USEPA, 2010). Furthermore, to validate that the final effluent is suitable for agricultural reuse, Table 1 outlines the discharge limits for non-food irrigation and food irrigation, demonstrating that effluent characteristics of CW-G-SSF and CW-MFC-GG-SSF is most appropriate for agriculture re-use.

3.5. Electricity generation in CW-MFC-GG

The voltage profile of CW-MFC-GG at 48 h is shown in Fig. 7a. At 48 h, variation in voltage was observed in the range of 518 ± 202.7 mV, and the highest voltage generation of 910 mV was observed. The substantial voltage at 48 h could be ascribed to enhanced ET from 16.37 ± 5.97 % (8 h) to 24.31 ± 8.89 % (48 h), respectively, as shown in Fig. 5d. This leads to high water loss, which augments the air-exposed cathode, thus increasing the O_2 concentration in the cathodic region (Mittal et al., 2023a; Srivastava et al., 2021c). This further improved the reaction kinetics by accelerating the electron flow from the anode to the cathode, thereby increasing voltage generation. In the present study, 700 Ω of internal resistance was estimated through a polarization curve with the highest current density and power density of 85.71 mA/m^3 and 25.71 mW/m^3, respectively (Fig. 7b). A similar finding reported internal resistance of 486.8 Ω in integrated vertical flow CW-MFC planted with *Canna indica* having an effective working volume of 11.5 L while treating swine wastewater (Liu et al., 2020).

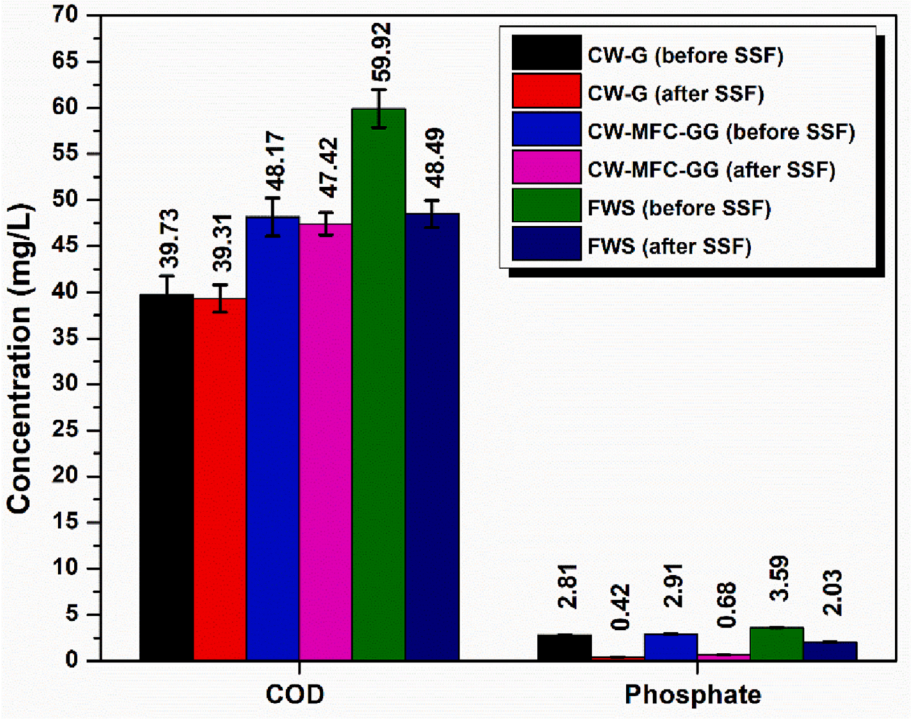

Fig. 6. COD and phosphate concentration before and after SSF treatment.

Table 1
Summarizes the characteristics of treated water in the present study and the limits for reuse in food and non-food crop irrigation purpose.

	Standard effluent discharge permissible limit	Food crop irrigation permissible limit	Non-food crop irrigation permissible limit	Effluent characteristics in present work	References
pH	6–9	6–9	6–9	CW-G-SSF; CW-MFC-GG-SSF; FWS-SSF Circumneutral (near to 7)	(Owusu-Ansah et al., 2015; Ritter, 2021)
COD	250 mg/L	≤40 mg/L	100 mg/L	CW-G-SSF: 39.31 mg/L CW-MFC-GG-SSF: 47.42 mg/L FWS-SSF: 48.49 mg/L	(Abdel-Shafy and Mansour, 2020; Owusu-Ansah et al., 2015; Rossi et al., 2021)
Phosphate	2 mg/L	0–2 mg/L	0–2 mg/L	CW-G-SSF: 0.42 mg/L CW-MFC-GG-SSF: 0.68 mg/L FWS-SSF: 2.03 mg/L	(Owusu-Ansah et al., 2015)
Turbidity	75 NTU	≤ 2 NTU	–	CW-G-SSF: 12.5 NTU CW-MFC-GG-SSF: 6 NTU FWS-SSF: 23 NTU	(Owusu-Ansah et al., 2015)
Total coliform	1000 CFU/100 mL	≤ 240 CFU/100 mL	–	CW-G-SSF: 221 CFU/100 mL CW-MFC-GG-SSF: 172 CFU/100 mL FWS-SSF: 542 CFU/100 mL	(Balkhair, 2016; Jeong et al., 2016)
Faecal coliform	<1000 CFU/100 mL	≤75 CFU/100 mL	200 CFU/100 mL (average)	CW-G-SSF: 0 CFU/100 mL CW-MFC-GG-SSF: 0 CFU/100 mL FWS-SSF: 240 CFU/100 mL	(Jeong et al., 2016; Owusu-Ansah et al., 2015; Ritter, 2021)
E. coli	<1000 CFU/100 mL	0 CFU/100 mL	≤200 CFU/100 mL (average)	CW-G-SSF: negative CW-MFC-GG-SSF: negative FWS-SSF: positive	(Jeong et al., 2016; Ritter, 2021)

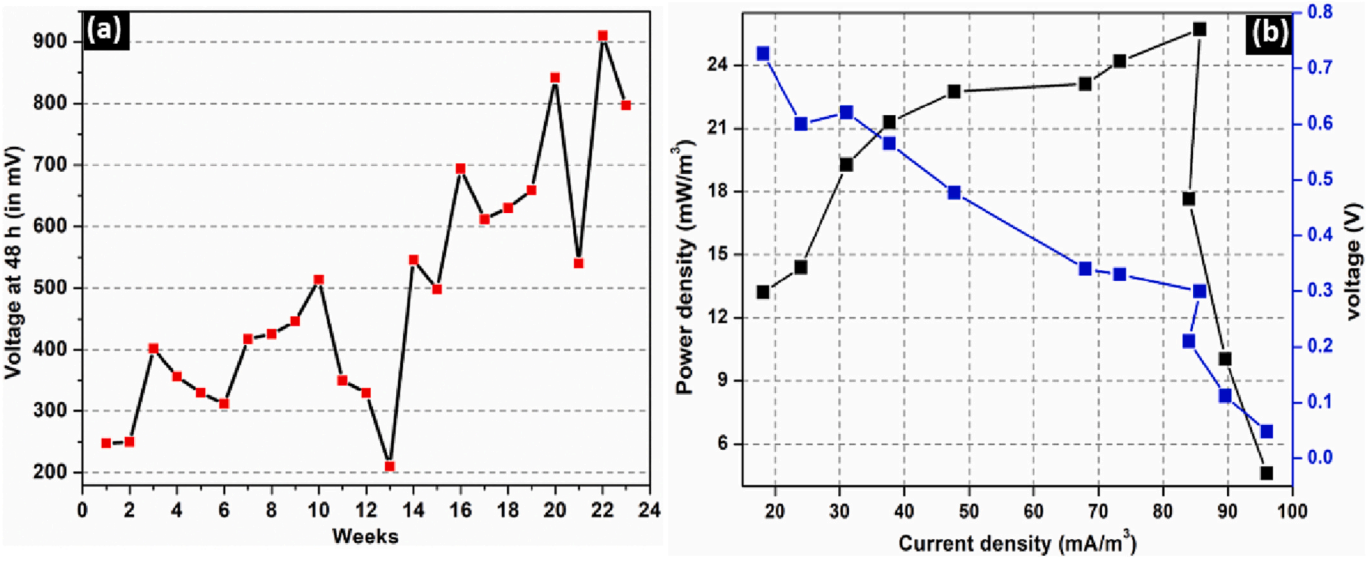

Fig. 7. (a) Voltage profile of CW-MFC-GG at 48 h throughout the course of study and (b) 48 h polarization curve of CW-MFC-GG.

4. Conclusion

The present research demonstrated promising results with a combination of CW-MFC-GG followed by SSF as secondary and tertiary wastewater treatment technology, respectively, in terms of total coliform, faecal coliform, *E. coli*, and turbidity removal. Whereas, treatment performance of the CW-MFC-GG microcosm was slightly lower than CW-G microcosm as a consequence of complex wastewater with a very low BOD/COD ratio. However, high volume reduction in CW-G indicates a high amount of sludge generation, suggesting early clogging, unstable long-term performance, and reduced life span in the long term. Nevertheless, both CW-G-SSF and CW-MFC-GG-SSF have fulfilled the standard discharge limits for COD and phosphate concentrations, and most significantly total coliform and faecal coliform number in the effluent pass the stringent regulations for reuse in agricultural purposes together with the absence of coliform *E. coli*. SSF as tertiary treatment has played a substantial role in achieving disinfection through a biologically active schmutzdecke layer, whereas wastewater treatment was mainly attained with secondary treatment technologies *i.e.*, CW-G, CW-MFC-GG, and FWS. Nonetheless, further research will be needed to optimize the systems in continuous mode, and life-cycle assessment studies of the integrated process for evaluating their sustainability.

CRediT authorship contribution statement

Yamini Mittal: Formal analysis, Validation, Investigation, Data curation, Visualization, Software, Methodology, Writing – original draft. **Pratiksha Srivastava:** Validation, Visualization, Writing – review & editing. **Sony Pandey:** Resources, Validation, Visualization. **Asheesh Kumar Yadav:** Conceptualization, Resources, Funding acquisition, Supervision, Methodology, Validation, Visualization, Writing – review & editing.

Declaration of competing interest

The authors declare the following financial interests/personal relationships which may be considered as potential competing interests: Asheesh Kumar Yadav reports a relationship with Council for Scientific

and Industrial Research (CSIR), India that includes: employment, and CSIR-IMMT and to CSIR India for granting Major Laboratory Project (MLP) number -037 and -059 as well as to DST India for granting grant number DST/TMD EWO/WTI/2K19/EWFH/2019/109.

Yamini Mittal reports GATE-SRF fellowship provided by the Council of Scientific and Industrial Research (CSIR), India.

Data availability

The authors do not have permission to share data.

Acknowledgment

YM acknowledges the GATE-SRF fellowship provided by the Council of Scientific and Industrial Research (CSIR), India. Asheesh Kumar Yadav acknowledges all the facilities and infrastructure provided by CSIR-IMMT and to CSIR India for granting grant numbers MLP-037 and MLP-059 as well as to DST India for granting fund (Grant number-DST/TMD EWO/WTI/2K19/EWFH/2019/109) for this research.

References

Abdel-Shafy, H.I., Mansour, M.S., 2020. Rehabilitation and upgrading wastewater treatment plant for safe irrigation reuse in remote area. Water Pract. Technol. 15, 1213–1227.

Ajonina, C., Buzie, C., Rubiandini, R.H., Otterpohl, R., 2015. Microbial pathogens in wastewater treatment plants (WWTP) in Hamburg. J. Toxicol. Environ. Health A 78, 381–387.

Alufasi, R., Gere, J., Chakauya, E., Lebea, P., Parawira, W., Chingwaru, W., 2017. Mechanisms of pathogen removal by macrophytes in constructed wetlands. Environ. Technol. Rev. 6, 135–144.

American Public Health Association, 2005. APHA (2005) Standard Methods for the Examination of Water and Wastewater. APHA Wash, DC USA.

Andreoli, F., Sabogal-Paz, L., 2020. Household slow sand filter to treat groundwater with microbiological risks in rural communities. Water Res. 186, 116352.

Ávila, C., Matamoros, V., Reyes-Contreras, C., Piña, B., Casado, M., Mita, L., Rivetti, C., Barata, C., García, J., Bayona, J.M., 2014. Attenuation of emerging organic contaminants in a hybrid constructed wetland system under different hydraulic loading rates and their associated toxicological effects in wastewater. Sci. Total Environ. 470–471, 1272–1280. https://doi.org/10.1016/j.scitotenv.2013.10.065.

Balkhair, K.S., 2016. Microbial contamination of vegetable crop and soil profile in arid regions under controlled application of domestic wastewater. Saudi J. Biol. Sci. 23, S83–S92.

Bolton, C.R., Randall, D.G., 2019. Development of an integrated wetland microbial fuel cell and sand filtration system for greywater treatment. J. Environ. Chem. Eng. 7, 103249.

CAWST, 2012. Biosand Filter Construction Manual.

Corbella, C., García, J., Puigagut, J., 2016a. Microbial fuel cells for clogging assessment in constructed wetlands. Sci. Total Environ. 569–570, 1060–1063. https://doi.org/10.1016/j.scitotenv.2016.06.163.

Corbella, C., Garfí, M., Puigagut, J., 2016b. Long-term assessment of best cathode position to maximise microbial fuel cell performance in horizontal subsurface flow constructed wetlands. Sci. Total Environ. 563, 448–455.

Deval, A.S., Parikh, H.A., Kadier, A., Chandrasekhar, K., Bhagwat, A.M., Dikshit, A.K., 2017. Sequential microbial activities mediated bioelectricity production from distillery wastewater using bio-electrochemical system with simultaneous waste remediation. Int. J. Hydrog. Energy 42, 1130–1141.

Du, L., Trinh, X., Chen, Q., Wang, C., Wang, H., Xia, X., Zhou, Q., Xu, D., Wu, Z., 2018. Enhancement of microbial nitrogen removal pathway by vegetation in Integrated Vertical-Flow Constructed Wetlands (IVCWs) for treating reclaimed water. Bioresour. Technol. 249, 644–651. https://doi.org/10.1016/j.biortech.2017.10.074.

Freitas, B.L.S., Terin, U.C., Fava, N. de M.N., Sabogal-Paz, L.P., 2021. Filter media depth and its effect on the efficiency of household slow sand filter in continuous flow. J. Environ. Manag. 288, 112412.

Gupta, S., Srivastava, P., Yadav, A.K., 2020. Simultaneous removal of organic matters and nutrients from high-strength wastewater in constructed wetlands followed by entrapped algal systems. Environ. Sci. Pollut. Res. 27, 1112–1117. https://doi.org/10.1007/s11356-019-06896-z.

Gupta, S., Mittal, Y., Panja, R., Prajapati, K.B., Yadav, A.K., 2021a. Conventional wastewater treatment technologies. Curr. Develop. Biotechnol. Bioeng. 47–75.

Gupta, S., Nayak, A., Roy, C., Yadav, A.K., 2021b. An algal assisted constructed wetland-microbial fuel cell integrated with sand filter for efficient wastewater treatment and electricity production. Chemosphere 263, 128132.

Gupta, S., Patro, A., Mittal, Y., Dwivedi, S., Saket, P., Panja, R., Saeed, T., Martínez, F., Yadav, A.K., 2023. The race between classical microbial fuel cells, sediment-microbial fuel cells, plant-microbial fuel cells, and constructed wetlands-microbial fuel cells: applications and technology readiness level. Sci. Total Environ. 879, 162757.

He, Y., Tao, W., Wang, Z., Shayya, W., 2012. Effects of pH and seasonal temperature variation on simultaneous partial nitrification and anammox in free-water surface wetlands. J. Environ. Manag. 110, 103–109.

Hejazi, M., Edmonds, J., Clarke, L., Kyle, P., Davies, E., Chaturvedi, V., Wise, M., Patel, P., Eom, J., Calvin, K., 2014. Long-term global water projections using six socioeconomic scenarios in an integrated assessment modeling framework. Technol. Forecast. Soc. Change 81, 205–226.

Iglesias, R., Ortega, E., Batanero, G., Quintas, L., 2010. Water reuse in Spain: data overview and costs estimation of suitable treatment trains. Desalination 263, 1–10.

ISI, 1982. Indian Standard: Methods of Sampling and Microbiological Examination of Water.

Jeong, H., Kim, H., Jang, T., 2016. Irrigation water quality standards for indirect wastewater reuse in agriculture: a contribution toward sustainable wastewater reuse in South Korea. Water 8, 169.

Kader Yettefti, I., Aboussabiq, F.E., Etahiri, S., Malamis, D., Assobhei, O., 2013. Slow sand filtration of effluent from an anaerobic denitrifying reactor for tertiary treatment: a comparable study, using three Moroccan sands. Carpathian J. Earth Environ. Sci. 8, 207–218.

Li, L., Yang, Y., Tam, N.F., Yang, L., Mei, X.-Q., Yang, F.-J., 2013. Growth characteristics of six wetland plants and their influences on domestic wastewater treatment efficiency. Ecol. Eng. 60, 382–392.

Liu, B., Lei, Y., Li, B., 2014. A batch-mode cube microbial fuel cell based "shock" biosensor for wastewater quality monitoring. Biosens. Bioelectron. 62, 308–314.

Liu, F., Sun, L., Wan, J., Shen, L., Yu, Y., Hu, L., Zhou, Y., 2020. Performance of different macrophytes in the decontamination of and electricity generation from swine wastewater via an integrated constructed wetland-microbial fuel cell process. J. Environ. Sci. 89, 252–263.

Mittal, Y., Dash, S., Srivastava, P., Mishra, P.M., Aminabhavi, T.M., Yadav, A.K., 2022. Azo dye containing wastewater treatment in earthen membrane based unplanted two chambered constructed wetlands-microbial fuel cells: a new design for enhanced performance. Chem. Eng. J. 427, 131856.

Mittal, Y., Noori, M.T., Saeed, T., Yadav, A.K., 2023a. Influence of evapotranspiration on wastewater treatment and electricity generation performance of constructed wetland integrated microbial fuel cell. J. Water Process Eng. 53, 103580.

Mittal, Y., Srivastava, P., Kumar, N., Kumar, M., Singh, S.K., Martinez, F., Yadav, A.K., 2023b. Ultra-fast and low-cost electroactive biochar production for electroactive-constructed wetland applications: a circular concept for plant biomass utilization. Chem. Eng. J. 452, 138587.

Mu, C., Wang, Lin, Wang, Li, 2021. Removal of Cr (VI) and electricity production by constructed wetland combined with microbial fuel cell (CW-MFC): influence of filler media. J. Clean. Prod. 320, 128860.

Narayan, M., Solanki, P., Srivastava, R.K., 2018. Treatment of sewage (domestic wastewater or municipal wastewater) and electricity production by integrating constructed wetland with microbial fuel cell. In: Sewage. IntechOpen.

Owusu-Ansah, E.de-G.J., Sampson, A., Amponsah, S.K., Abaidoo, R.C., Hald, T., 2015. Performance, Compliance and Reliability of Waste Stabilization Pond: Effluent Discharge Quality and Environmental Protection Agency Standards in Ghana.

Ranjan, P., Prem, M., 2018. Schmutzdecke-a filtration layer of slow sand filter. Int. J. Curr. Microbiol. Appl. Sci. 7, 637–645.

Ritter, W., 2021. State regulations and guidelines for wastewater reuse for irrigation in the US. Water 13, 2818.

Rossi, G., Mainardis, M., Aneggi, E., Weavers, L.K., Goi, D., 2021. Combined ultrasound-ozone treatment for reutilization of primary effluent—a preliminary study. Environ. Sci. Pollut. Res. 28, 700–710.

Saeed, T., Majed, N., Yadav, A.K., Hasan, A., Miah, M.J., 2022. Constructed wetlands for drained wastewater treatment and sludge stabilization: role of plants, microbial fuel cell and earthworm assistance. Chem. Eng. J. (Lausanne, Switzerland: 1996) 430, 132907.

Saket, P., Mittal, Y., Bala, K., Joshi, A., Kumar Yadav, A., 2021. Innovative constructed wetland coupled microbial fuel cell for enhancing diazo dye degradation with simultaneous electricity generation. Bioresour. Technol., 126490 https://doi.org/10.1016/j.biortech.2021.126490.

Samantray, P., Mishra, B.K., Panda, C.R., Rout, S.P., 2009. Assessment of water quality index in Mahanadi and Atharabanki Rivers and Taldanda Canal in Paradip area, India. J. Hum. Ecol. 26, 153–161.

Saz, Ç., Türe, C., Türker, O.C., Yakar, A., 2018. Effect of vegetation type on treatment performance and bioelectric production of constructed wetland modules combined with microbial fuel cell (CW-MFC) treating synthetic wastewater. Environ. Sci. Pollut. Res. 25, 8777–8792.

Seeger, E.M., Braeckevelt, M., Reiche, N., Müller, J.A., Kästner, M., 2016. Removal of pathogen indicators from secondary effluent using slow sand filtration: optimization approaches. Ecol. Eng. 95, 635–644.

Shingare, R.P., Thawale, P.R., Raghunathan, K., Mishra, A., Kumar, S., 2019. Constructed wetland for wastewater reuse: role and efficiency in removing enteric pathogens. J. Environ. Manag. 246, 444–461.

Srivastava, P., Yadav, A.K., Garaniya, V., Abbassi, R., 2019. Constructed wetland coupled microbial fuel cell technology: development and potential applications. In: Microbial Electrochemical Technology. Elsevier, pp. 1021–1036.

Srivastava, P., Abbassi, R., Yadav, A., Garaniya, V., Asadnia, M., Lewis, T., Khan, S.J., 2021a. Influence of applied potential on treatment performance and clogging behaviour of hybrid constructed wetland-microbial electrochemical technologies. Chemosphere 284, 131296. https://doi.org/10.1016/j.chemosphere.2021.131296.

Srivastava, P., Abbassi, R., Yadav, A.K., Garaniya, V., Lewis, T., Zhao, Y., Aminabhavi, T., 2021b. Interrelation between Sulphur and conductive materials and its impact on ammonium and organic pollutants removal in electroactive wetlands. J. Hazard. Mater. 419 https://doi.org/10.1016/j.jhazmat.2021.126417.

Srivastava, P., Belford, A., Abbassi, R., Asadnia, M., Garaniya, V., Yadav, A.K., 2021c. Low-power energy harvester from constructed wetland-microbial fuel cells for initiating a self-sustainable treatment process. Sustain. Energy Technol. Assess. 46 https://doi.org/10.1016/j.seta.2021.101282.

Tamta, P., Rani, N., Mittal, Y., Yadav, A.K., 2023. Evaluating the potential of multi-anodes in constructed wetlands coupled with microbial fuel cells for treating wastewater and bioelectricity generation under high organic loads. Energies 16. https://doi.org/10.3390/en16020784.

Taskan, E., Hasar, H., 2015. Comprehensive comparison of a new tin-coated copper mesh and a graphite plate electrode as an anode material in microbial fuel cell. Appl. Biochem. Biotechnol. 175, 2300–2308. https://doi.org/10.1007/s12010-014-1439-4.

Torrens, A., Molle, P., Boutin, C., Salgot, M., 2009. Removal of bacterial and viral indicator in vertical flow constructed wetlands and intermittent sand filters. Desalination 246, 169–178. https://doi.org/10.1016/j.desal.2008.03.050.

Tyagi, V.K., Khan, A.A., Kazmi, A.A., Mehrotra, I., Chopra, A.K., 2009. Slow sand filtration of UASB reactor effluent: a promising post treatment technique. Desalination 249, 571–576. https://doi.org/10.1016/j.desal.2008.12.049.

United States, Environmental Protection Agency, Office of Wastewater Management, Municipal Support Division, National Risk Management Research Laboratory (US), Technology Transfer, Support Division, 2004. Guidelines for Water Reuse. US Environmental Protection Agency.

USEPA, 2010. NPDES Permit Writers' Manual.

Verma, S., Daverey, A., Sharma, A., 2017. Slow sand filtration for water and wastewater treatment–a review. Environ. Technol. Rev. 6, 47–58.

Weber-Shirk, M.L., Dick, R.I., 1997. Physical-chemical mechanisms in slow sand filters. Am. Water Works Assoc. J. 89, 87.

World Health Organization, 2006. WHO Guidelines for the Safe Use of Wasterwater Excreta and Greywater. World Health Organization.

Xu, L., Wang, B., Liu, X., Yu, W., Zhao, Y., 2018a. Maximizing the energy harvest from a microbial fuel cell embedded in a constructed wetland. Appl. Energy 214, 83–91.

Xu, L., Zhao, Y., Tang, C., Doherty, L., 2018b. Influence of glass wool as separator on bioelectricity generation in a constructed wetland-microbial fuel cell. J. Environ. Manag. 207, 116–123.

Xu, F., Ouyang, D., Rene, E.R., Ng, H.Y., Guo, L., Zhu, Y., Zhou, L., Yuan, Q., Miao, M., Wang, Q., Kong, Q., 2019. Electricity production enhancement in a constructed wetland-microbial fuel cell system for treating saline wastewater. Bioresour. Technol. 288, 121462 https://doi.org/10.1016/j.biortech.2019.121462.

Yadav, A., 2010. Design and Development of Novel Constructed Wetland Cum Microbial Fuel Cell for Electricity Production and Wastewater Treatment, pp. 4–10.

Yang, Y., Zhan, X., Wu, S., Kang, M., Guo, J., Chen, F., 2016. Effect of hydraulic loading rate on pollutant removal efficiency in subsurface infiltration system under intermittent operation and micro-power aeration. Bioresour. Technol. 205, 174–182.

Yang, Y., Zhao, Y., Tang, C., Xu, L., Morgan, D., Liu, R., 2020. Role of macrophyte species in constructed wetland-microbial fuel cell for simultaneous wastewater treatment and bioenergy generation. Chem. Eng. J. 392, 123708 https://doi.org/10.1016/j.cej.2019.123708.

Yang, Y., Zhao, Y., Tang, C., Liu, R., Chen, T., 2021. Dual role of macrophytes in constructed wetland-microbial fuel cells using pyrrhotite as cathode material: a comparative assessment. Chemosphere 263, 128354.

Yang, R., Liu, M., Yang, Q., 2022. Microbial fuel cell affected the filler pollution accumulation of constructed wetland in the lab-scale and pilot-scale coupling reactors. Chem. Eng. J. 429, 132208.

Zhang, Z., Rengel, Z., Meney, K., 2009. Kinetics of ammonium, nitrate and phosphorus uptake by Canna indica and Schoenoplectus validus. Aquat. Bot. 91, 71–74. https://doi.org/10.1016/j.aquabot.2009.02.002.

Zhao, Y., Collum, S., Phelan, M., Goodbody, T., Doherty, L., Hu, Y., 2013. Preliminary investigation of constructed wetland incorporating microbial fuel cell: batch and continuous flow trials. Chem. Eng. J. 229, 364–370.

Zhao, C., Shang, D., Zou, Y., Du, Y., Wang, Q., Xu, F., Ren, L., Kong, Q., 2020. Changes in electricity production and microbial community evolution in constructed wetland-microbial fuel cell exposed to wastewater containing Pb(II). Sci. Total Environ. 732, 139127 https://doi.org/10.1016/j.scitotenv.2020.139127.

Zhou, M., Chi, M., Luo, J., He, H., Jin, T., 2011. An overview of electrode materials in microbial fuel cells. J. Power Sources 196, 4427–4435. https://doi.org/10.1016/j.jpowsour.2011.01.012.

Zurita, F., Carreón-Álvarez, A., 2015. Performance of three pilot-scale hybrid constructed wetlands for total coliforms and Escherichia coli removal from primary effluent–a 2-year study in a subtropical climate. J. Water Health 13, 446–458.